Kidney International, Vol. 59 (2001), pp. 554–564

Flow cytometric immunodissection of the human distal tubule and cortical collecting duct system

MARK J.F. HELBERT, SIMONNE E.H. DAUWE, and MARC E. DE BROE

Department of Nephrology, University of Antwerp, Belgium

Flow cytometric immunodissection of the human distal tubule and cortical collecting duct system.

Background. In recent years, considerable efforts were drawn to isolate human distal tubule (DT) and collecting duct (CD) cells with more or less success. Here, we present a procedure for isolating human DT cells [thick ascending limb (TAL)/distal convoluted tubule (DCT)] and CD system cells (connecting tubule/initial CD) as separate populations within the same kidney specimen, applying monoclonal antibodies in fluorescence-activated cell sorting (FACS) and culturing them.

Methods. We tested antibodies directed against the DT/CD system antigens, epithelial membrane antigen (EMA) and L1-cell adhesion molecule (L1-CAM). Segmental and subsegmental expressions were first assessed by using morphologic and histotopographic criteria, and by comparing sections with adjacent sections stained for expression of well-defined distal subsegment-specific markers. Immunoreactive cells were further characterized by dual immunostaining using cell type-specific markers. As a second step, cells obtained by collagenase digestion of normal renal cortical tissue were flow sorted following labeling with aforementioned antibodies and cultured.

Results. EMA expression was found on all cells present in the DT and in the CD system. Its expression was most abundant in TAL and from thereon decreased gradually along the course of the DT and CD system. Flow sorting of all EMA-expressing cells resulted in identification/isolation of DT and CD system cells as a heterogeneous mixture. Flow sorting of only the most strongly EMA-positive cells allowed purification of DT cells only, mainly TAL cells as shown by Tamm-Horsfall protein expression on >80% of sorted cells. L1-CAM was expressed in only the CD system, and sorting of all L1-CAM–positive cells allowed >95% purification of CD system cells (connecting tubule/cortical CD). Primary cultures of DT and CD system cells rapidly developed into confluent monolayers, and retained antigenic and functional properties inherent to their segments of origin.

Conclusion. Our study presents a procedure for isolating and culturing pure populations of human DT cells and CD system cells as separate populations, using antibodies to the best available markers in FACS.

Key words: cell culture, fluorescence activated cell sorting, epithelial membrane antigen, L1-cell adhesion molecule, markers to isolate cells, tubular cell pathology.

Received for publication April 5, 2000
and in revised form July 10, 2000
Accepted for publication August 25, 2000

Human tubular cell pathophysiology is often studied using cultured cells, as the in vitro approach generally avoids the complexity of whole-organ/whole-animal experiments. Whereas a vast amount of information has been obtained on proximal tubule (PT) cell physiology using PT cells in primary culture, data concerning distal tubule (DT)/collecting duct (CD) cells are more limited. The DT and the (cortical) CD system consist of an array of at least five ultrastructurally distinct cell types [thick ascending limb (TAL) cells, distal convoluted tubule (DCT) cells, connecting tubule cells, principal cells, and at least two types of intercalated cells (IC cells)], which are topographically organized into one or more subsegments [TAL, DCT, connecting tubule (CT), and CD] [1]. In all species that have been studied, including human, the TAL and the initial DCT are clearly marked off from one another and contain exclusively TAL cells and DCT cells, respectively [2, 3]. The remaining subsegments (late DCT, CT, CD) are much less clearly marked off from one another except in a minority of species such as guinea pig and rabbit. In the latter, each subsegment is characterized by the presence of its specific cell type(s): late DCT, DCT cells only; CT, CT cells, and IC cells; CD, principal cells, and IC cells [4]. In most other species, including humans, transitional zones of variable length exist between these consecutive subsegments in which aforementioned cell types are intermingled [1, 5]. Consequently, some portions of the (late) DT and initial CD system may contain up to four different cell types. This in vivo heterogeneity has been shown to be reflected in similar in vitro heterogeneity in the event of starting off cell cultures from these segments obtained by microdissection in rabbits [5] and humans [6]. To overcome the difficulties associated with heterogeneous cultures, several investigators have used permanent cell lines exhibiting properties suggestive of either DT or CD origin [such as the Madin Darby canine kidney (MDCK; dog), OK (opossum), JCT-12 (cynomolgus monkey), and A6 (*Xenopus laevis*) cell lines]. Following extensive characterization, however, most cell lines show an ambiguous phenotype. The widely used MDCK cells, for example,

express a furosemide-sensitive $Na^+/K^+/2\ Cl^-$ symporter (consistent with TAL origin), but show a hormonal profile consistent with CD origin [7, 8]. Another approach was the development of immortalized cell lines via transformation of primary cells by introducing defined oncogenes into cells of defined segment origin. This led to the development of a mouse DT (MDCT) and inner medullary CD cell line (mIMCD-K2) and of several rabbit cell lines [RC.SV2 (TAL origin), RC.SV3 and RC.SVtsA58 (principal cell origin), as well as RCCT-28 A (β-IC cell origin)] retaining several characteristics of their segments of origin [9–15]. Several studies, however, discourage the widespread use of immortalized cell lines, as loss of cell differentiation [16, 17], development of ambiguous "hybrid" phenotypes [18], and persistent heterogeneity despite repeated subcloning [19] seem common drawbacks of cell immortalization.

Until now, the methods described for obtaining primary cultures of purified DT/CD cells are macroseparation techniques, microdissection and immunodissection. Macroseparation techniques use differential sieving and/or (Percoll®/Ficoll®) gradient centrifugation for purification of enzyme-dispersed tubular cells/segments prior to bringing them into culture. Such preparative techniques have been described for obtaining DT-, CT-, and CD-enriched segments in rabbits [20, 21], but not humans. Several groups have used the microdissection approach to isolate and purify individual subsegments leading to pure cultures of TAL cells, DCT cells and/or CT/CD cells in rats, rabbits [5, 22–25], and humans [6, 26, 27]. Manual microdissection allows high-grade purification, but the cell yield is relatively low. Immunodissection techniques, applying antibodies/lectins [panning, magnetic (MACS) and fluorescence-activated cell sorting (FACS)], generally allow purification of larger cell numbers and have been used for isolating TAL cells, IC cells, and CT/CD cells in several animal species [28–34]. FACS has also been used for obtaining TAL cells and heterogeneous DT/CD cultures in humans [35–37]. To date, immunodissection of human DT and CD system cells as separate populations from a single kidney specimen was not possible because of the lack of surface markers, of which the expression is limited to either DT or CD system. Due to the development of new monoclonal antibodies with powerful immunoselection potential, this has changed. We present a flow cytometric technique that allows simultaneous purification (and culture) of human DT cells (TAL/DCT) and CD system cells (CT/cortical CD) as separate viable populations.

METHODS

Immunoperoxidase staining

An overview of antibodies used in immunohistochemistry (and FACS) is shown in Table 1. Moab 272 [anti-L1 cell adhesion molecule (anti-L1-CAM)] was a kind gift of P.M. Ronco. MoAb 272 was originally developed using an immortalized rabbit CD cell line as immunogen. It was found to react with a basolateral epitope present on CT and CD principal cells in rabbits and humans [13, 38]. Later, the antigen was characterized as being an isoform of (brain) cell adhesion molecule L1 (abstract; Debiec et al, *J Am Soc Nephrol* 63: 374, 1995). MoAb AD-1 [antileucine aminopeptidase (anti-LAP)] and MoAb 7E8 were characterized in this lab [39, 40]. The remaining antisera were obtained from a commercial source.

To study the expression of antigens in the DT/CD system, we performed immunoperoxidase staining on formol-calcium–fixed paraffin sections of normal human kidney tissue (unaffected pole of tumor nephrectomy specimen) as described previously [37]. Staining patterns for all surface markers were studied in at least four different kidney specimens. For (sub)segment identification of tubules in kidney sections, we used morphologic criteria (PT: periodic acid-Schiff–positive brush border), histotopographic criteria (TAL/OSOM-CD: localization within medullary rays), and immunologic criteria [comparison of sections with adjacent sections stained for epidermal growth factor (EGF) immunoreactivity and for Tamm-Horsfall protein (THP)]. THP immunostaining permits the identification of TALs and initial DCTs [37, 42–44]. Nouwen and De Broe demonstrated that EGF immunostaining using polyclonal AB-3 results in distinct cellular staining patterns in different (sub)segments [TAL, predominant apical surface staining; DCT, cytoplasmic staining; early and late CT, staining equally distributed over the entire cell surface on $>75\%$ and $<50\%$ of cells per tubular cross section, respectively; cortical CDs, $<10\%$ of cells per tubule cross section with basal cell surface staining (octopal cells)] [43]. For cell phenotype identification in CT and CD, sections were double immunostained for L1-CAM and for either carbonic anhydrase type II (CA-II; reported earlier to be expressed most abundantly by IC cells in the CT and initial CD) [45, 46] or the basolateral chloride/bicarbonate anion exchanger AE-1 (proposed marker for type A IC cells) [47, 48]. The first primary antibody (anti–L1-CAM) was detected using a biotinilated horse anti–mouse-specific secondary antibody and avidin/biotin/alkaline phosphatase complex (both from Vector, Burlingame, CA, USA). Alkaline phosphatase staining was developed using nitrobluetetrazolium (Sigma Chemical Co., St. Louis, MO, USA) as staining reagent and 5-bromo-4-chloro-3-indoxyl-phosphate (Sigma) as substrate. Next, the section was preincubated with 20% (vol/vol) mouse serum followed by incubation with the second primary antibody (sheep-anti-carbonic anhydrase/rabbit-anti-AE-1, respectively), after which endogenous peroxidase activity was blocked. The second primary antibody was visualized using a peroxidase-conjugated secondary antibody (rabbit anti-sheep/

Table 1. Overview of antibodies used in immunohistochemistry, immunocytochemistry and flow-sorting experiments

	Antigen	Abbreviation	EC NR	Clone	Host	Reference
Proximal	Leucine aminopeptidase	LAP	3.4.11.1	AD-1	Mouse IgG_1	[39]
Distal tubular/ collecting duct	Epithelial membrane antigen	EMA		MGRM/5/11/I-CR2	Rat IgG_{2a}	Sera-lab
				E29	Mouse IgG_{2a}	DAKO
				E29	Mouse IgG_{2a}-peroxidase	DAKO
	Tamm-Horsfall protein	THP			Sheep polyclonal	Chemicon
					Goat polyclonal	Organon
	L1-cell adhesion molecule	L1-CAM		272	Mouse IgG	[18, 38]
	(recombinant) Epidermal growth factor	EGF		AB-3	Rabbit polyclonal	Oncogene science
Epithelial	Human cytokeratin (type 5, 6, 8 and 17)			MNF-116	Mouse IgG-peroxidase	DAKO
Intercalated cell	Cl^-/HCO_3^--anion exchanger	AE-1		MSDBIII	Rabbit polyclonal	[41]
	Carbonic anhydrase	CA-II	4.2.1.1.		Sheep polyclonal	Biodesign International
Isotype control	Placental alkaline phosphatase	PLAP	3.1.3.1.	7E8	Mouse IgG_1	[40]
	Glucose oxidase				Mouse IgG-peroxidase	DAKO

donkey anti-rabbit, respectively; Amersham, Arlington Heights, IL, USA). All cross-reactivity with (mouse)-anti-L1-CAM and (horse)-anti-mouse was removed from the peroxidase-conjugated secondary antibody by prediluting it in mouse and horse serum.

Quantitation of immunohistochemical staining by digital image analysis

As epithelial membrane antigen (EMA) immunostaining resulted in heterogeneous staining intensities throughout the DT and the CD system, its expression in different subsegments was quantitated and compared using digital image analysis. Equipment consisted of the Kontron KS 400 V2.00 digital imaging system and software (Kontron Elektronik, München, Germany) connected to a Leica DMR-B microscope. TAL, DCT, early and late CT, and CD cross sections (20 each) were selected blindly on adjacent sections stained for EGF immunoreactivity according to aforementioned staining criteria. No more than three tubular cross-sections were chosen per (×200) microscope field to limit the amount of cross sections originating from a single tubule. A region bordered by the tubular cell bases and cell apices was drawn interactively in the video image and the area of the resulting region [tubular cell area (TCA)] was measured in pixels. The abundance of immunostaining in each tubular cross section was then expressed as the percentage of TCA that stained positively (TCA%). TCA% was calculated as the ratio of the amount of pixels with density value > highest density value of the appropriate negative control section (primary antibody omitted) over the total number of pixels present in TCA. Data are presented graphically as box-whisker plots. Statistical analysis was performed using Systat®. Since values were not normally distributed (Lilliefors test for hypothesis that data are from a normal distribution), overall comparisons were evaluated by Kruskal–Wallis one-way analysis of variance (ANOVA). Individual comparisons were made by Mann–Whitney *U* test, and a *P* value of 0.0055 was considered significant.

Preparation of a single cell suspension

Cells were obtained from tumor nephrectomy specimens. The use of the latter was approved by our local ethical committee. A sample for histologic assessment was collected to confirm absence of pathological tissue in the used (unaffected) pole. Briefly, tissue from cortex and outer stripe of outer medulla was dissected and cut into pieces of ± 1 mm^3. Tissue pieces were resuspended in collagenase solution and subjected to three subsequent 30-minute digestions as extensively described [37]. The cell suspensions were sieved through a 50 μm mesh sieve, washed in M199 + 5% (vol/vol) fetal calf serum (FCS) and centrifuged on top of a discontinuous Percoll® gradient (densities of 1.07, 1.05, and 1.04 g/mL) to eliminate debris [37]. All material from the intersection 1.05 to 1.07 to the intersection 1.04 to 1.05 was collected and washed.

Cell labeling and cell sorting

Cells were labeled in 5% (vol/vol) FCS-supplemented M199 medium (0.5 to 1.0 × 10^6 cells/100 μL). Primary antibodies were added in optimal amounts as determined by titration against a fixed number of cells. Primary antibody was omitted in control samples. After one hour of incubation, cells were washed (120 g, 7 min) with 3 mL phosphate-buffered saline (PBS) supplemented with 1% FCS. Subsequently, samples were incubated for 30 minutes with phycoerythrinated/fluoresceinated rabbit $F(ab')_2$ anti-mouse IgG (RAM), or fluoresceinated $F(ab')_2$ goat anti-rat IgG.

The labeled cells were analyzed and sorted using a FACSSTAR^{PLUS} sorter (BDIS) equipped with an argon-ion laser tuned to 488 nm at 40 mW power. Data were

processed with the Lysis II analysis program (BDIS). Positively labeled cells were identified by their fluorescence over that of the appropriate control sample. When fluorescence histograms revealed a population of fluorescing cells well separated from a second peak of cells showing fluorescence intensities not higher than those of the control sample, the percentage of positively labeled cells was defined as the percentage showing higher fluorescence intensities than the intensity corresponding to the trough of the fluorescence intensity distribution.

To verify precision of sorting, over 1000 sorted cells were re-analyzed for fluorescence intensity. To check for their origin, cells were also sorted directly onto poly L-lysine–coated microscope slides and air dried for LAP cytochemical staining (indicating PT origin) [37] and cytokeratin and EMA immunostaining (indicating epithelial and DT or CD origin, respectively). EMA and cytokeratin staining were performed using peroxidase-conjugated anti-EMA and anticytokeratin antibodies. These were prevented from binding to fluorochrome-conjugated RAM by preincubating the cell slides with 20% mouse serum. We tested the possibility of enriching the sorted population with TAL/DCT cells by limiting the sorted population to the more strongly EMA-expressing cells. For this purpose, we defined sort gates through which all EMA positive cells were sorted (100%) as well as sort gates through which only the 50, 33, 25, 10, and 5% most positive cells of the entire EMA-positive subset were sorted, respectively. The amount of immunocytochemically THP-positive cells (THP being present on TAL and initial DCT cells) in these gated subsets was then taken as measure for their enrichment with DT cells. For the purpose of counting the THP-positive percentage, gated cells were sorted directly onto microscope slides and were air dried. Following pretreatment with 20% (vol/vol) goat serum in PBS (30 minutes), they were incubated with biotinilated (goat-)anti-THP, avidin/biotin/peroxidase complex, and 3-amino-9-ethylcarbazole chromagen (AEC).

Cell viability was checked following incubation of cells with propidium iodide [49, 50].

Characterization of cultured cells: Antigen expression and hormonal stimulation

Following sorting, cells were seeded at a density of approximately 0.5×10^5 cells/mL MEM-α medium modified according to Gibson-d'Ambrosio supplemented with 10% (vol/vol) heat-inactivated FCS [51]. Surface antigen expression was measured flow cytometrically in >80% confluent passage 0 cultures following trypsinization [0.12% trypsin/0.02% ethylenediaminetetraacetic acid (EDTA), 5 minutes] and labeling as described for gradient-purified cells. Hormonal stimulation of adenylate cyclase was started once passage 1 cells had regained >80% confluence (day 9). Minimal essential medium (MEM) (GIBCO, Grand Island, NY, USA) containing 0.5 mmol/L isobutylmethylxanthine (IBMX) and human parathyroid hormone (PTH, 300 nmol/L; Sigma) or arginine-vasopressin (AVP, 1000 nmol/L; Boehringer Mannheim, Mannheim, Germany) was added for 150 minutes. Stimulation was stopped by removing the medium. Basal cAMP production was measured by exposing cells to MEM + IBMX. cAMP was measured using an immunoassay (determinations in duplicate; R&D Systems, Minneapolis, MN, USA). Cell protein was determined by the bicinchoninic acid (BCA) method. Results are expressed as fmol cAMP/μg protein (mean ± SD, 5 cultures from 3 kidneys). Differences versus control were identified by Student *t* test.

RESULTS

Surface marker distribution along the nephron

Epithelial membrane antigen. EMA immunoreactivity was found on all cells of the DT and the CD systems (Fig. 1). Expression was limited to the apical cell surface except for CT and CD in which a minority of cells showed additional weak cytoplasmic staining. Apical staining intensity was variable in different distal (sub)segments, and digital image analysis (Fig. 2) revealed that EMA was expressed most strongly in TALs, followed by (in order of staining intensity) DCTs, early CTs, late CTs, and CDs ($P < 0.0055$ for all comparisons except for late CT vs. CD, $P = 0.007$, borderline significant). Cells in PTs, thin limbs, glomeruli, and interstitium were all EMA negative.

L1-CAM. Serial sections revealed L1-CAM expression to be present in CT and cortical/outer medullary CD and to be absent in PTs, DTs, glomeruli, and the interstitium (Fig. 3). In early CT, L1-CAM staining was limited to a subset of cells (59 ± 6% of total) at their basal cell surface and demonstrated a speckled linear staining pattern (Fig. 3G). In CD, staining was again present on a subset of cells (61 ± 7%); here, basal cell surface staining was more abundant, and additional strong staining was present on the lateral cell surface (Fig. 3H). Tangential sections revealed L1-CAM–positive cells to have a polygonal outline except where juxtaposed to "rounded" L1-CAM–negative cells (showing a typical oval outline with a more or less round basolateral pole), in which case they seemed to support the latter (Fig. 3H, arrow). Next to these rounded L1-CAM–negative cells, a minority of L1-CAM–negative cells showed polygonal morphology. Double staining for L1-CAM and AE-1 (marker for type A IC cells) always demonstrated mutually exclusive expression on individual cells (Fig. 4A), compatible with the principal cell nature of L1-CAM–positive cells. Double staining was also performed for L1-CAM and CA-II (reported earlier to be expressed most abundantly by IC cells in CT/CD), and L1-CAM–

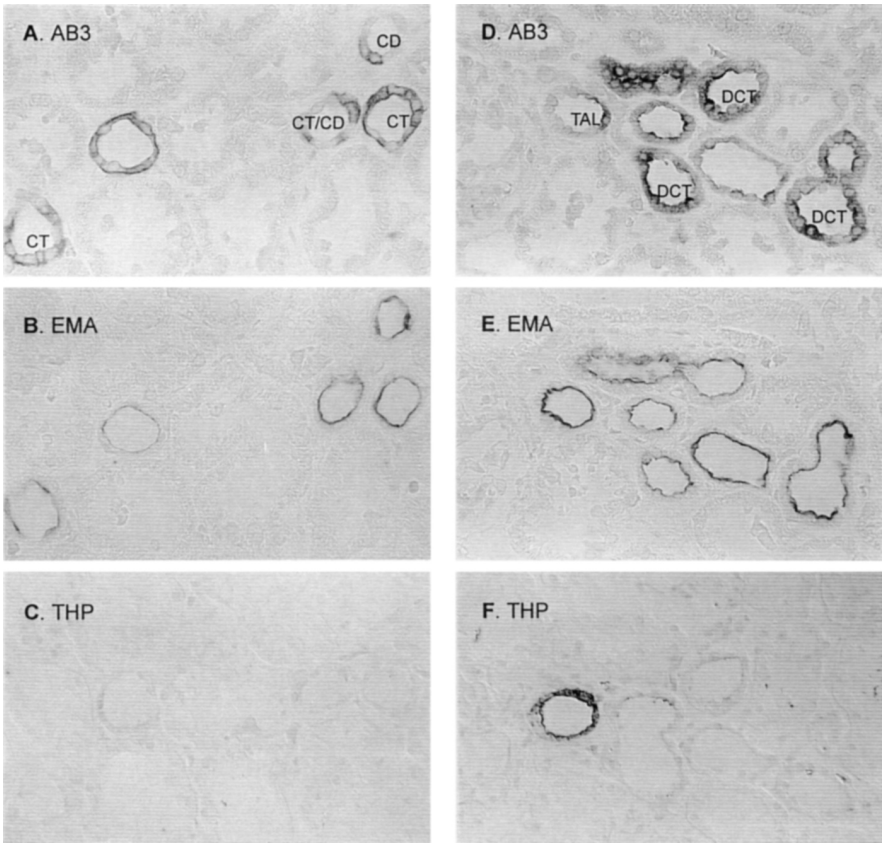

Fig. 1. Segmental and (sub)segmental expression of epithelial membrane antigen (EMA) in human kidney. Serial sections were stained for epidermal growth factor (EGF) immunoreactivity (*A* and *D*), allowing identification of tubular cross sections as thick ascending limb (TAL), distal convoluted tubule (DCT), connecting tubule (CT) or cortical collecting duct (CD) cells, EMA immunoreactivity (*B* and *E*) and the TAL/initial DCT marker THP (*C* and *F*). The description of staining patterns is described in the text (original magnifications ×200).

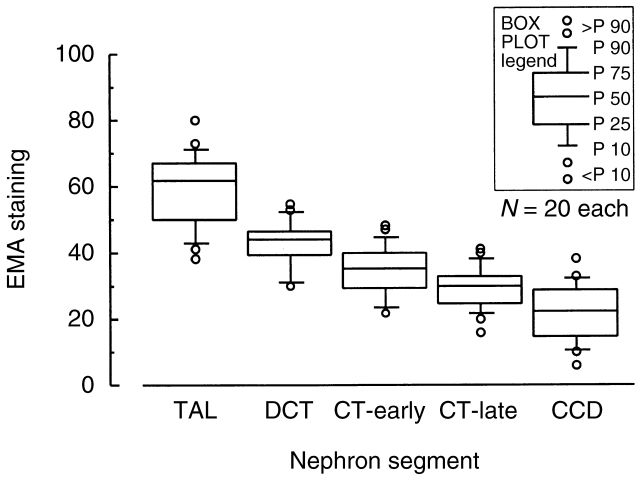

Fig. 2. Comparison of EMA immunostaining in human DT and CD system subsegments. Staining was quantitated by digital-image analysis. Abundance of immunostaining was calculated as the percentage of tubular cell area that stained positively (TCA%). Values of different subsegments are presented as box-whisker plots. Abbreviations are: TAL, thick ascending limb; DCT, distal convoluted tubule; CT-early, early connecting tubule; CT-late, late connecting tubule; and CD, collecting duct.

positive cells were found to show variable CA-II immunoreactivity (Fig. 4B). Interestingly, L1-CAM/CA-II dual staining also revealed the presence of double-negative cells, indicating that not all IC cells are CA-II positive (Fig. 4B).

Flow cytometric analysis of gradient-purified cell suspensions

Flow cytometric analysis of samples incubated with anti-EMA and anti–L1-CAM always resulted in a population of highly fluorescent cells (Fig. 5A, B), with fluorescence intensities well above those of the appropriate control samples (primary antibody omitted; Fig. 5C). On the other hand, labeling cells with sheep/goat polyclonal anti-THP never resulted in a positive signal in FACS (Fig. 5D).

Anti-EMA, shown on sections to be expressed on all DT/CD cells resulted in the highest number of positively labeled cells (25 ± 8%, $N = 11$). Accuracy of sorting was assessed by a re-analysis of sorted cells using flow cytometry without changing the instrument settings. Reanalysis always revealed a population of >95% highly fluorescent cells (Fig. 5E). When EMA-positive cells were sorted directly onto microscope slides for immunocytochemical purposes, staining for presence of LAP, cytokeratin, and EMA confirmed their DT/CD origin

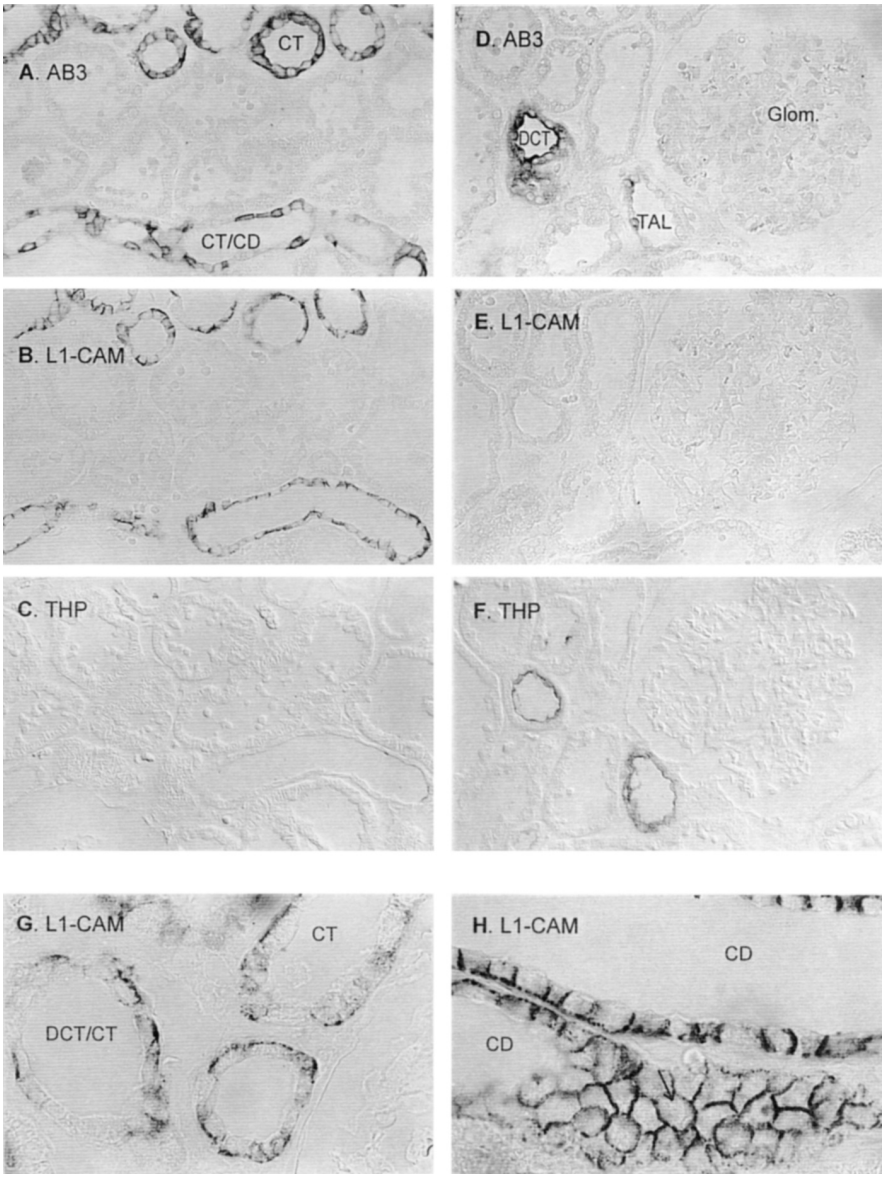

Fig. 3. Segmental and subsegmental expression of L1-CAM in human kidney. Serial sections were stained for EGF immunoreactivity (*A* and *D*), allowing identification of tubular cross-sections as TAL, DCT, CT, or C-CD, L1-CAM immunoreactivity (B and E) and for the TAL/initial DCT marker THP (*C* and *F*). The description of staining patterns is discussed in the text. L1-CAM immunostaining is less abundant in the (initial) CT (*G*) when compared with late CT and C/OM-CD (*H*). Tangential sections reveal that L1-CAM–positive cells have a polygonal morphology except when supporting neighboring oval/round-shaped (L1-CAM negative) cells (arrow in H; original magnifications: A–F, ×200; G–H, ×600).

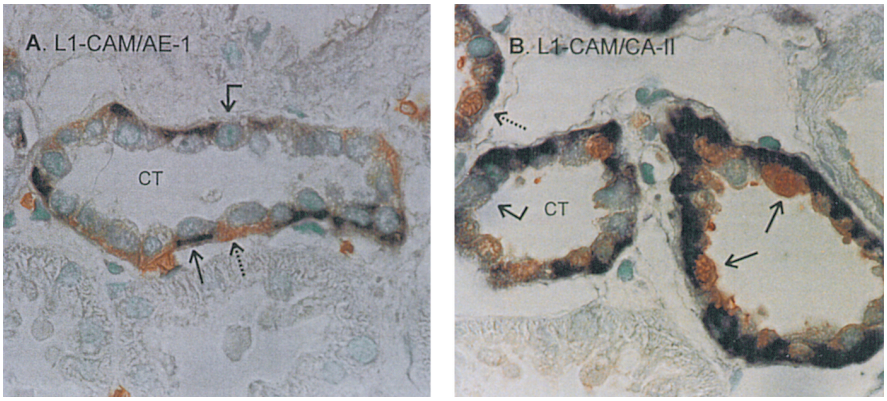

Fig. 4. Light micrographs of dual-immunostained sections. The section in (*A*) was stained for L1-CAM [developed with alkaline phosphatase (black), black arrow] and chloride/bicarbonate anion exchanger AE-1 [developed with peroxidase (red), dotted arrow] and illustrates mutual exclusive expression of both differentiation antigens on one and the same cell. Dual-negative cells (↵) are DCT cells or non–A-type IC cells. The section in (*B*) was stained for L1-CAM (developed with alkaline phosphatase, black) and carbonic anhydrase type II (developed with peroxidase, red) and illustrates that (*1*) carbonic anhydrase expression is present in L1-CAM–negative cells (dotted arrow), but is not limited to L1-CAM–negative cells (black arrows), and (*2*) that not all L1-CAM–negative cells express carbonic anhydrase (↵).

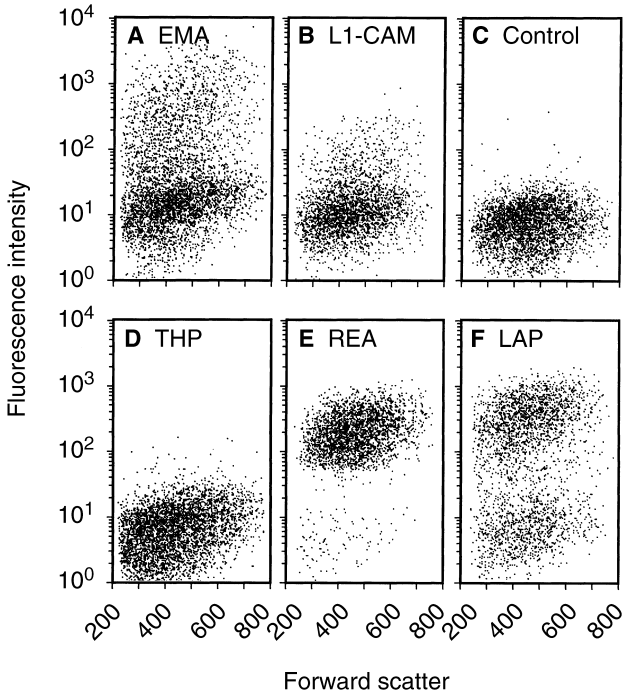

Fig. 5. Forward scatter (horizontal axis) vs. fluorescence intensity (vertical axis) dot plots of unsorted cell samples from one and the same human kidney labeled for expression of the DT/CD system marker EMA (*A*), the CD system marker L1-CAM (*B*), the TAL/initial DCT marker THP (*D*), and the PT marker LAP (*F*). (*C*) Control sample, primary antibody omitted. (*E*) Re-analysis sample.

(Table 2). Flow cytometric analysis of dual-labeled samples confirmed mutually exclusive expression of EMA and LAP on individual cells (data not shown).

Anti–L1-CAM (Fig. 5B) clearly resulted in labeling of fewer cells (6 ± 2%, $N = 12$). Staining of L1-CAM–positive cells sorted directly onto microscope slides showed them to be cytokeratin positive, EMA positive, and LAP negative (Table 2). The absence of THP expressing cells in the L1-CAM–positive sorted population (0.5 ± 1%, $N = 5$), as opposed to presence of a considerable percentage of THP-expressing cells in the EMA-positive sorted population (29 ± 8%, $N = 5$), confirmed the CT/CD origin of L1-CAM–positive sorted cells (Table 2). L1-CAM/LAP dual labeling also demonstrated the L1-CAM–positive cells not to be LAP positive (data not shown).

Since digital imaging showed EMA to be expressed more strongly in the DT than in the CD system, we attempted to enrich the sorted population with DT (TAL/DCT) cells by selecting only the strongly EMA-expressing cells. For this purpose, gates in the fluorescence intensity histogram were constructed that enabled us to sort populations containing the 50, 33, 25, 10, and 5% most strongly EMA-expressing cells of the entire EMA-positive subset (Fig. 6A). By limiting the sorted population from all EMA expressing cells to only the 5% most strongly EMA-positive cells, the THP-positive percentage (THP being present only on TAL cells and initial DCT cells) increased from 29.6 ± 8.1% to 77.7 ± 5.7% ($N = 5$; Fig. 6B), indicating that selecting only the more strongly EMA expressing cells indeed results in purification of DT cells (TAL enriched).

Viability of sorted cells (measured as percentage cells excluding PI in FACS) was 73 ± 3% (mean ± SD, $N = 3$).

Distal tubule versus collecting duct cells in culture

Within 24 hours after sorting, DT cells (sorted on the basis of belonging to the 10% most strongly EMA expressing cells) and CT/CD cells (sorted on the basis of L1-CAM expression) began to adhere; outgrowth became apparent after 48 hours. Cells grew confluent within five to seven days. In phase-contrast microscopy, DT and CT/CD monolayers could not be distinguished from one another, as both consisted of closely packed curvilinear cells with limited granularity (as compared with more polygonal outline and higher granularity of proximal cells). After 10 to 12 days of confluency, dome formation was observed in both culture types.

Figure 7 shows antigen expression in (passage 0, day 8) confluent DT and CT/CD cultures, as determined by FACS. DT cells continue to express higher EMA levels than CT/CD cells. Similarly, CT/CD cells continue to express L1-CAM in culture, whereas DT cells never express L1-CAM.

Figure 8 illustrates the hormonal stimulation of cAMP production in heterogeneous DT/CD system cultures [obtained by sorting all EMA expressing cells (100%)], DT cultures (obtained by sorting only the 10% most strongly EMA expressing cells), CD system cultures (obtained by sorting all L1-CAM–positive cells), PT cultures (obtained by sorting LAP-positive cells), and mixed cultures (previously unsorted cells). cAMP production in previously unsorted cultures showed both a PTH- (95-fold basal, $P < 0.05$) and an AVP-sensitive (30-fold basal, $P < 0.05$) increase. cAMP production in heterogeneous DT/CD system cultures showed a strong PTH- (450-fold basal, $P < 0.05$), as well as a strong AVP-sensitive (140-fold basal, $P < 0.05$) increase. cAMP production in DT cell cultures showed a very strong PTH-sensitive increase (1100-fold basal, $P < 0.05$), whereas the AVP response was clearly weaker (90-fold basal, $P < 0.05$). On the other hand, cAMP production in CT/CD system cultures showed a very strong AVP-sensitive increase (820-fold basal, $P < 0.05$), whereas PTH resulted in a smaller increase (70-fold basal, $P < 0.05$). Finally, proximal cultures showed a significant increase following PTH stimulation (>100-fold basal, $P < 0.05$), unlike following AVP stimulation (P = NS).

Table 2. Percentages of cytokeratin, LAP, EMA and THP positive cells following sorting for expression of various surface markers

Sorted population	% cytokeratin positive (epithelial)	% LAP positive (proximal)	% EMA positive (DT/CD)	% THP positive (DT)
EMA+	94 ± 3 ($N = 5$)	2 ± 2 ($N = 8$)	95 ± 2 ($N = 5$)	29 ± 8 ($N = 5$)
L1-CAM+	98 ± 1 ($N = 4$)	1 ± 1 ($N = 6$)	95 ± 3 ($N = 5$)	0.5 ± 1 ($N = 5$)
LAP+		95 ± 3 ($N = 5$)		

Over 2000 cells were sorted onto poly-L-lysine coated microscope slides based on expression above control of several DT and/or CD markers and the proximal marker LAP. Sorted cells were stained cytochemically for presence of LAP and immunocytochemically for expression of cytokeratin, EMA and THP. Abbreviations are in Table 1.

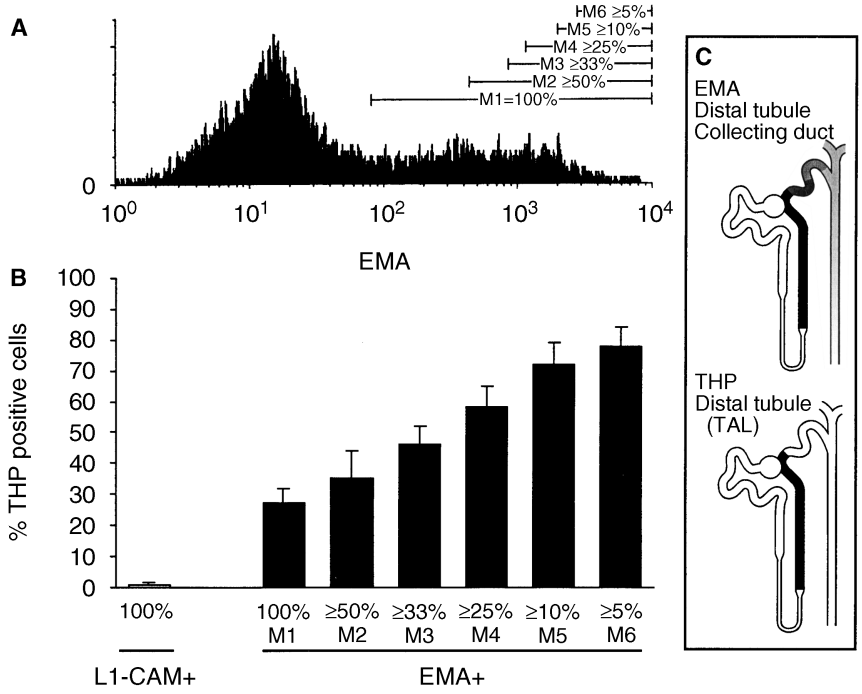

Fig. 6. Flow sorting of human DT cells. (*A*) Fluorescence intensity histogram of the population prior to sorting following labeling with anti-EMA. M1 represents the sort gate containing the entire EMA-positive subpopulation (100%). M2 through M6 represent electronic sort gates containing the 50, 33, 25, 10, and 5% most positive cells of the entire EMA-positive subset, respectively. (*B*) Illustrates the percentages of THP positive cells present in the populations obtained following sorting of EMA positive cells through aforementioned gates (M1 through M6) and the percentage of THP-positive cells in the L1-CAM–positive sorted cells (mean ± SD, $N = 5$ different kidney specimens). (*C*) Schematically illustrates expression of EMA (maximal in TAL and from thereon decreasing along the course of the DT and CD, hence useful as a tool for sorting DT cells) and of THP (present in only TAL/initial DCT, hence useful as a parameter for assessing DT origin of sorted cells).

DISCUSSION

This study shows which surface markers can be used for flow cytometric purification and subsequent culture of human DT and CD system cells as separate populations from a single kidney specimen. When applied on cells naturally occurring as part of a solid organ, FACS purification implies a thorough tissue dispersion procedure. Surface markers may be lost during this procedure because of exposition to (exogenous/endogenous) enzymes, shedding following cell–cell dissociation, internalization following interaction with ligands, and/or epitope instability [37, 52, 53]. In this way, THP, although present abundantly on TAL cells in vivo, proved inappropriate for FACS of TAL cells.

The majority of surface markers expressed in the DT are also expressed in the CD system and vice versa. This was also the case for EMA, which was expressed on the entire variety of cells present in the DT (TAL cells/DCT cells) and CD system (CT cells/CD cells). Flow sorting of the entire EMA positive population resulted in >95% purification of DT/CD system cells. The heterogeneous nature of the resulting population was underscored by the presence of THP (TAL/initial DCT marker) on approximately 30% of sorted cells. Quantitation of immunostaining by digital imaging analysis demonstrated EMA expression to be most abundant in the TAL, diminishing gradually from that point along the course of the DT and CD system. Accordingly, narrowing of the sorted population from all EMA-positive cells to only the 5% most strongly EMA-expressing cells resulted in an immunoselection of DT cells, up to 80% enriched with TAL/initial DCT cells, as demonstrated by THP immuno reactivity. No further increase of the THP-positive percentage was obtained by enforcing more rigorous sorting criteria. This is probably due to an overlap of EMA expression intensities on TAL/initial DCT cells (both THP positive) and late DCT cells (THP negative).

Immunohistochemically, expression of L1-CAM was limited to connecting tubules and CDs. The ratio of L1-CAM–positive/L1-CAM–negative cells in these segments

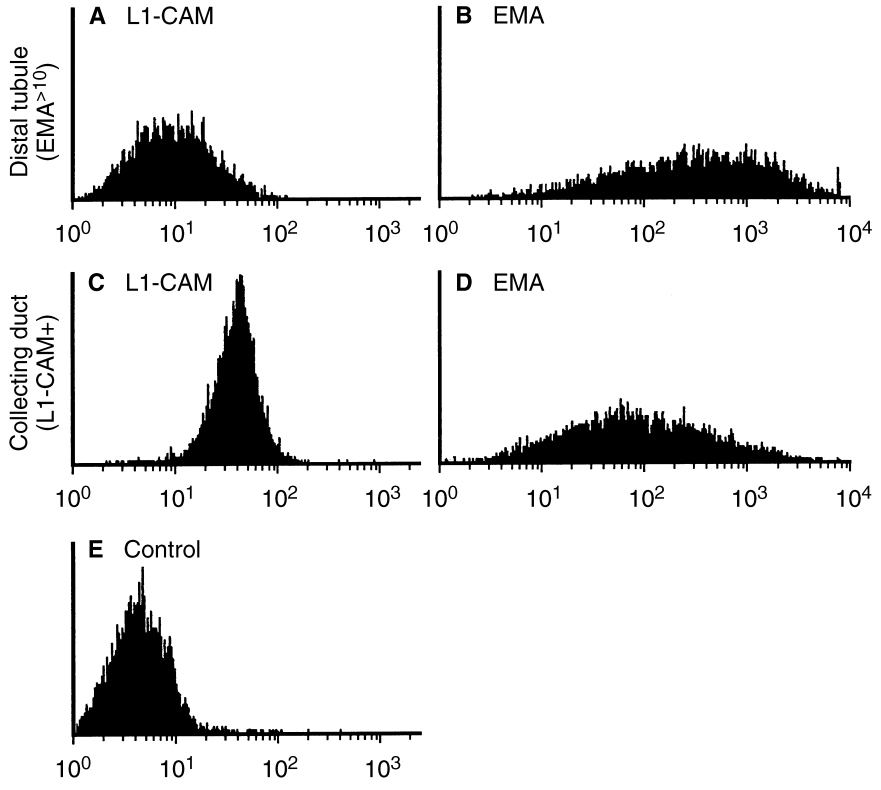

Fig. 7. Fluorescence histograms comparing the expression of L1-CAM (*A* and *C*) and EMA (*B* and *D*) on cultured human DT (*A* and *B*) and CD system (*C* and *D*) cells. Expression was analyzed in >80% confluent passage 0 cells (culture day 8). DT cells were originally sorted from a fresh kidney specimen based on high expression of EMA (10% most EMA-positive cells); CD cells were sorted based on L1-CAM expression. Histogram in (*E*) represents negative control (primary omitted).

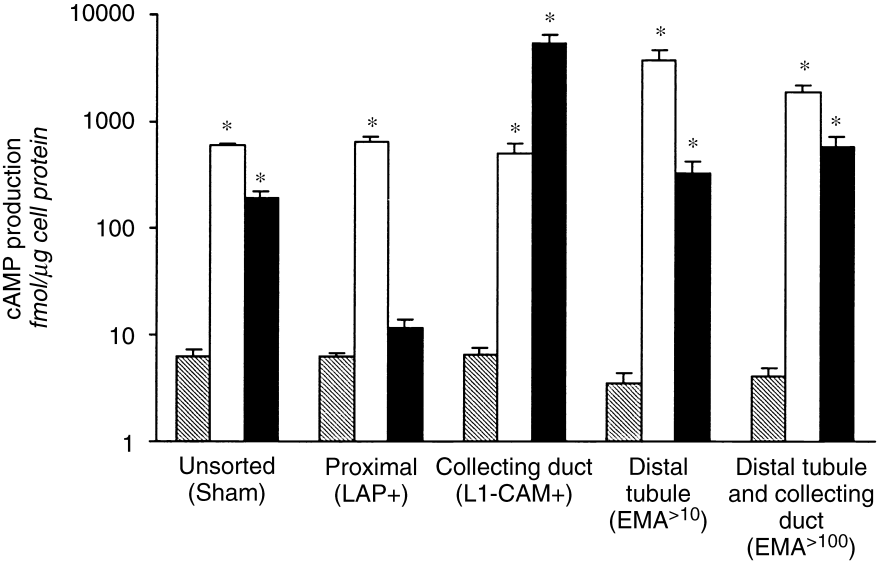

Fig. 8. Comparison of cAMP production following hormonal stimulation of human proximal, distal, CD and sham-sorted cultures. Proximal cells, DT cells, and CD system cells were sorted from a fresh kidney specimen based on expression of LAP, high expression of EMA (10% most EMA positive cells), and expression of L1-CAM, respectively. Cultures containing DT and CD cells as a heterogeneous mixture (but not proximal cells) were obtained by sorting all EMA positive cells (100%). Sham-sorted cultures were run through the cytometer without undergoing any selection (= unsorted sample). cAMP production was measured in >80% confluent passage 1 cells (day 9) following stimulation with PTH (300 nmol/L) and AVP (1000 nmol/L). Basal cAMP production was measured by exposing cells to medium (MEM) devoid of hormones. Results are expressed as fmol cAMP per μg cell protein (mean ± SD, $N = 5$ different cultures derived from three kidney specimens). Note the logarithmic scale. Symbols are: (▨) MEM; (□) PTH; (■) AVP; $*P < 0.05$ vs. control.

was approximately 3:2, which is very similar to the principal cell/IC cell ratios described earlier in these segments in rats and rabbits [3, 4, 54, 55]. Morphologically, L1-CAM–positive cells presented with a polygonal/cubical outline (as described for connecting tubule and principal cells), whereas the majority of L1-CAM–negative cells presented with a rounded/oval outline (as described for a subset of IC cells) [1, 43, 56]. The more or less discontinuous "speckled" L1-CAM staining pattern on the basal plasma membrane can be explained by a restriction of L1-CAM expression to the plasma membrane where not in contact with the basement membrane, as described earlier in rabbit principal cells [38]. The CT/principal cell nature of L1-CAM–positive cells was corroborated

further by the mutually exclusive expression of L1-CAM and the type A IC cell marker AE-1. We occasionally observed strong CA-II expression on L1-CAM–positive cells, confirming the aforementioned observation that in humans (as in mice and rats but unlike in rabbits), strong CA-II immunoreactivity is not limited to CT/CD IC cells [45, 46, 57]. On the other hand, the presence of L1-CAM/CA-II dual-negative cells in the CT indicates that (at least in human) CA-II is not expressed by all IC cells. Indeed, CA-II/AE-1 dual labeling confirmed that more than half of the type A IC were CA-II negative (not shown).

Flow sorting of L1-CAM–positive cells resulted in isolation of >95% pure CD system cells. Sorting of all L1-CAM–positive cells and only the most strongly EMA-expressing cells following L1-CAM/EMA dual labeling appeared an elegant and efficient method for simultaneous isolation of DT (TAL/DCT) and CD system (CT/CD) cells as separate populations from a single kidney specimen. We calculated that our method allows isolation of approximately 0.25×10^4 DT cells and 0.5×10^4 CD system cells per gram of kidney tissue. Although aforementioned immunostaining results seem to support principal cell nature of the L1-CAM–positive cells, it is unlikely that the L1-CAM–positive sorted population is entirely devoid of IC cells, since the gradient purified fraction is not a true single-cell suspension and contains a substantial amount of tubular "fragments" consisting of up to two or three cells. As soon as IC cell markers applicable in flow become available, it will become possible to sort out any contaminating IC cells.

Viability following sorting was as high as 70% when measured by propidium iodide exclusion, and cells grew into confluent monolayers within six to eight days. DT and CT/CD cells retained differentiation characteristics once in culture such as high EMA expression and L1-CAM expression, respectively. Both showed distinct hormonal responsiveness patterns: DT cells showed a strong PTH-sensitive increase of adenylate cyclase activity, whereas CT/CD cells showed a strong AVP-sensitive increase. These patterns are entirely in accordance with those found for microdissected rabbit and human DT and CD system segments and with PTH/AVP receptor localization studies [25, 27, 58, 59]. Dome formation was observed in both DT and CT/CD cultures, indicating the presence of tight cell junctions and transepithelial transport.

In conclusion, FACS allows (simultaneous) isolation of pure populations of cells of DT and CD system origin. Both cell types grow into homogeneous monolayers and retain in vivo characteristics such as antigen profile and cAMP response to PTH and AVP. These cultures will be of use in studying cell biology, pathophysiology, and electrophysiology of DT and CD system cells.

ACKNOWLEDGMENTS

M. Helbert is a recipient of the research grant "aspirant" of the National Fund for Scientific Research (Nationaal Fonds voor Wetenschappelijk Onderzoek). The authors express their gratitude to Dirk De Weerdt for the illustrations and Erik Snelders for help with the manuscript. This work would not have been possible without the kind cooperation of the urologists and staff of the hospitals affiliated with the Antwerp University Hospital.

Reprint requests to Marc E. De Broe, M.D., Ph.D., University of Antwerp, Department of Nephrology-Hypertension, p/a University Hospital Antwerp, Wilrijkstraat 10, B-2650 Edegem/Antwerpen, Belgium. E-mail: snelders@uia.ua.ac.be

APPENDIX

Abbreviations used in this article are: anti-LAP, antileucine aminopeptidase; AVP, arginine vasopressin; CA-II, carbonic anhydrase type II; CAM, cell adhesion molecule; CCD, cortical collecting duct; CD, collecting duct; CT, connecting tubule; DCT, distal convoluted tubule; DT, distal tubule; EGF, epidermal growth factor; EMA, epithelial membrane antigen; FACS, fluorescence activated cell sorting; IBMX, isobutylmethylxanthine; IC, intercalated cells; L1-CAM, L1-cell adhesion molecule; PT, proximal tubule; PTH, parathyroid hormone; TAL, thick ascending limb; TCA, tubular cell area; THP, Tamm-Horsfall protein.

REFERENCES

1. Kriz W, Kaissling B: Structural organization of the mammalian kidney, in *The Kidney: Physiology and Pathophysiology*, edited by Seldin DW, Giebisch G, New York, Raven Press, 1985, pp 265–306
2. Tisher CC, Madsen KM: Anatomy of the kidney, in *The Kidney* (3rd ed), edited by Brenner BM, Philadelphia, W.B. Saunders, 1986, pp 3–60
3. Crayen ML, Thoenes W: Architecture and cell structures in the distal nephron of the rat kidney. *Cytobiology* 17:197–211, 1978
4. Kaissling B, Kriz W: Structural analysis of the rabbit kidney. *Adv Anat Embryol Cell Biol* 56:1–123, 1979
5. Wilson PD, Anderson RJ, Breckon RD, *et al:* Retention of differentiated characteristics by cultures of defined rabbit kidney epithelia. *J Cell Physiol* 130:245–254, 1987
6. Wilson PD, Dillingham MA, Breckon R, *et al:* Defined renal tubular epithelia in culture: growth, characterization, and hormonal response. *Am J Physiol* 248:F436–F443, 1985
7. Saier MH: Growth and differentiated properties of a kidney epithelial cell line. *Am J Physiol* 240:C106–C109, 1981
8. Louvard D: Apical membrane aminopeptidase appears at site of cell-cell contact in cultured kidney epithelial cells. *Proc Natl Acad Sci USA* 77:4132–4136, 1980
9. Vandewalle A, Lelongt B, Geniteau-Legendre M, *et al:* Maintenance of proximal and distal functions in SV-40-transformed tubular cell lines derived from rabbit kidney cortex. *J Cell Physiol* 141:203–221, 1989
10. McDonald C, Watts P, Stuart B, *et al:* Studies on the phenotype and karyotype of immortalized rabbit kidney epithelia cell lines. *Exp Cell Res* 195:458–461, 1991
11. Vandewalle A, Ronco PM, Cassingena R: Establishment of permanent renal tubular cell lines by infection with the wild type and a thermosensitive mutant of the Simian Virus SV-40. *Am J Kidney Dis* 17:619–621, 1991
12. Dai LJ, Friedman PA, Quamme GA: Phosphate depletion diminishes Mg^{2+}-uptake in mouse distal convoluted tubule cells. *Kidney Int* 51:1710–1718, 1997
13. Prie D, Dussaule JC, Lelongt B, *et al:* Principal cell-specific antigen and hormonal regulatory network in RC.SVtsA58 cell line. *Am J Physiol* 266:C1628–C1638, 1994
14. Gesek FA, Friedman PA: On the mechanism of parathyroid hormone stimulation of calcium uptake by mouse distal convoluted tubule cells. *J Clin Invest* 90:749–758, 1992

15. Kizer NL, Lewis B, Stanton BA: Electrogenic sodium absorption and chloride secretion by an inner medullary collecting duct cell line (mIMCD-K2). *Am J Physiol* 268:F347–F355, 1995
16. Charlton JA, Simmons NL: Established human renal cell lines: Phenotypic characteristics define suitability for use in in vitro models for predictive toxicology. *Toxic Vitro* 7:129–136, 1993
17. Teulon J, Ronco PM, Geniteau-Legendre M, *et al:* Transformation of renal tubule epithelial cells by Simian Virus-40 is associated with emergence of Ca^{2+}-insensitive K^+ channels and altered mitogenic sensitivity to K^+ channel blockers. *J Cell Physiol* 151:113–125, 1992
18. Prie D, Dussaule J-C, Lelongt B, *et al:* Principal-cell specific antigen and hormonal regulatory network in RC.SVtsA58 cell line. *Am J Physiol* 266:C1628–C1638, 1994
19. Nakazato Y, Suzuki H, Saruta T: Characterizations of subclones of Madin Darby canine kidney renal epithelial cell line. *Biochim Biophys Acta* 1014:57–65, 1989
20. Bello-Reus E, Weber MR: Electrophysiological studies of primary cultures of rabbit distal tubule cells. *Am J Physiol* 252:F899–F909, 1987
21. Lajeunesse D, Regnier L, Thales S, *et al:* Simultaneous isolation and biochemical characterization of connecting and collecting tubules by ficoll gradient. *Kidney Int* 47:306–311, 1995
22. Aigner J, Kloth S, Kubitza M, *et al:* Maturation of renal collecting duct cells in vivo and under perfusion culture. *Epithelial Cell Biol* 3:70–78, 1994
23. Merot J, Bidet M, Gachot B, *et al:* Electrical properties of rabbit early distal convoluted tubule in primary culture. *Am J Physiol* 257:F288–F299, 1989
24. White S, Reeve H: Primary culture of collecting duct cell epithelium from neonate rabbit kidney in monolayer. *Exp Physiol* 77:129–139, 1992
25. Chabardes D, Imbert M, Clique A, *et al:* PTH sensitive adenyl cyclase activity in different segments of the rabbit nephron. *Pflügers Arch* 354:229–239, 1975
26. Trifillis AL, Kahn MW: Characterization of an in vitro system of human renal papillary collecting duct cells. *In Vitro Cell Dev Biol* 26:441–446, 1990
27. Chabardes D, Gagnan-Brunette M, Imbert-Teboul M, *et al:* Adenylate cyclase responsiveness to hormones in various portions of the human nephron. *J Clin Invest* 65:439–448, 1980
28. Bacskai BJ, Friedman PA: Activation of latent Ca^{2+}-channels in renal epithelial cells by parathyroid hormone. *Nature* 347:388–391, 1990
29. Rose UM, Hartog A, Jansen JW, *et al:* Anoxia-induced increases in intracellular calcium concentration in primary cultures of rabbit thick ascending limb of Henle's loop. *Biochem Biophys Acta* 1226: 291–299, 1994
30. Bindels RJ, Hartog A, Timmermans J, *et al:* Active Ca^{2+} transport in primary cultures of rabbit kidney CCD: Stimulation by 1,25-dihydroxyvitamin D3 and PTH. *Am J Physiol* 261:F799–F807, 1991
31. Allen ML, Nakao A, Sonnenburg WK, *et al:* Immunodissection of cortical and medullary thick ascending limb cells from rabbit kidney. *Am J Physiol* 255:F704–F710, 1988
32. Spielman WS, Sonnenburg WK, Allen ML, *et al:* Immunodissection and culture of rabbit cortical collecting tubule cells. *Am J Physiol* 251:F348–F357, 1986
33. Pizzonia JH, Gesek FA, Kennedy SM, *et al:* Immunomagnetic separation, primary culture and characterization of cortical thick ascending limb plus distal convoluted tubule cells from mouse kidney. *In Vitro Cell Dev Biol* 27A:409–416, 1991
34. Fejes-Toth G, Naray-Fejes-Toth A: Isolated principal and intercalated cell hormone responsiveness and Na^+-K^+-ATPase activity. *Am J Physiol* 256:F742–F750, 1989
35. Baer PC, Nocker WA, Haase W, *et al:* Isolation of proximal and distal tubule cells from human kidney by immunomagnetic separation. *Kidney Int* 52:1321–1331, 1997
36. Van Der Biest I, Nouwen EJ, Van Dromme SA, *et al:* Characterization of pure proximal and heterogeneous distal human tubular cells in culture. *Kidney Int* 45:85–94, 1994
37. Helbert MJF, Dauwe SEH, Vanderbiest I, *et al:* Immunodissection of the human proximal nephron: Flow sorting of S1S2S3, S1S2 and S3 proximal tubular cells. *Kidney Int* 52:414–428, 1997
38. Prie D, Friedlander G, Coureau C, *et al:* Role of adenosine on glucagon-induced cAMP in a human cortical collecting duct cell line. *Kidney Int* 47:1310–1318, 1995
39. Deng JT, Hoeylaerts MF, Nouwen EJ, *et al:* Purification of liver plasma membrane fragments using a monoclonal anti-leucine aminopeptidase. *Hepatology* 23:445–454, 1996
40. Nouwen EJ, Pollet DE, Eerdekens MW, *et al:* Immunohistochemical localisation of placental alkaline phosphatase, carcinoembryonic antigen, and cancer antigen 125 in normal and neoplastic human lung. *Cancer Res* 46:866–876, 1986
41. Drenckhahn D, Merte C: Restriction of the human kidney band 3-like anion exchanger to specialized subdomains of the basolateral plasma membrane of intercalated cells. *Eur J Cell Biol* 45:107–115, 1987
42. Kumar S, Muchmore A: Tamm-Horsfall protein: Uromodulin (1950-1990). *Kidney Int* 37:1395–1401, 1990
43. Nouwen EJ, De Broe ME: EGF and TGF-alpha in the human kidney: Identification of octopal cells in the collecting duct. *Kidney Int* 45:1510–1521, 1994
44. Nadasdy T, Laszik Z, Blick KE, *et al:* Human acute tubular necrosis: A lectin and immunohistochemical study. *Hum Pathol* 26:230–239, 1995
45. Spicer SS, Sens MA, Tashian RE: Immunocytochemical demonstration of carbonic anhydrase in human epithelial cells. *J Histochem Cytochem* 30:864–873, 1982
46. Loennerholm G, Wistrand PJ: Carbonic anhydrase in the human kidney: A histochemical and immunohistochemical study. *Kidney Int* 25:886–898, 1984
47. Godinich MJ, Jennings ML: Renal chloride-bicarbonate exchangers. *Curr Opin Nephrol Hypertens* 4:398–401, 1995
48. Wagner S, Vogel R, Lietzke R, *et al:* Immunochemical characterization of a band 3-like anion exchanger in collecting duct of human kidney. *Am J Physiol* 253:F213–F221, 1987
49. Carter NP: Measurement of cellular subsets using antibodies, combined antibody/fluorochrome techniques, in *Flow Cytometry*, edited by Ormerod MG, Oxford, Oxford University Press, 1990, pp 45–68
50. Nieminen A-L, Gores GJ, Daqwson TL, *et al:* Toxic injury from mercuric chloride in rat hepatocytes. *J Biol Chem* 265:2399–2408, 1990
51. Gibson-d'Ambrosio RE, Samuel M, Chang CC, *et al:* Characteristics of long-term human epithelial cell cultures derived from normal human fetal cells. *In Vitro* 23:279–287, 1983
52. Biddlestone LR, Fleming S: Calcium dependence of A-CAM function in human renal epithelium. *J Pathol* 166:163–169, 1992
53. Jalkaenen M, Rapraeger A, Saunders S, *et al:* Cell surface proteoglycan of mouse mammary epithelial cells is shed by cleavage of its matrix-binding ectodomain from its membrane associated domain. *J Cell Biol* 105:3087–3096, 1987
54. Welling LW, Evan AP, Welling DJ, *et al:* Morphometric comparison of rabbits cortical connecting tubules and collecting ducts. *Kidney Int* 23:358–367, 1983
55. Hansen GP, Tisher CC, Robinson RR: Response of the collecting duct to disturbances of acid base and potassium balance. *Kidney Int* 17:326–337, 1980
56. Kim J, Tischer CC, Madsen KM: Differentiation of intercalated cells in developing rat kidney: An immunohistochemical study. *Am J Physiol* 35:F977–F990, 1994
57. Dobyan DC, Magill LS, Friedman PA, *et al:* Carbonic anhydrase histochemistry in rabbit and mouse kidneys. *Anat Rec* 204:185–197, 1982
58. Lee K, Brown D, Urena P, *et al:* Localization of parathyroid hormone/parathyroid hormone-related peptide receptor mRNA in kidney. *Am J Physiol* 270:F186–F191, 1996
59. Terada Y, Tomita K, Nonoguchi H, *et al:* Different localization and regulation of two types of vasopressin receptor messenger RNA in microdissected rat nephron segments using reverse transcription polymerase chain reaction. *J Clin Invest* 92:2339–2345, 1993